Biosensors and Bioelectronics 142 (2019) 111518

Contents lists available at ScienceDirect

Biosensors and Bioelectronics

journal homepage: www.elsevier.com/locate/bios

A simple approach to quantitative determination of soluble amyloid-β peptides using a ratiometric fluorescence probe

Changhong Li[a], Liu Yang[a], Yuwang Han[a], Xiaohui Wang[a,b,*]

[a] College of Chemistry and Molecular Engineering, Nanjing Tech University, Nanjing, 211816, PR China
[b] State Key Laboratory of Coordination Chemistry, Nanjing University, Nanjing, 210093, PR China

ARTICLE INFO

Keywords:
Alzheimer's disease
Soluble Aβ
Ratiometric fluorescence probe
Quantitative detection
Zn^{2+}-mediated recognition

ABSTRACT

Alzheimer's disease (AD) is a progressive neurodegenerative illness that affects the elderly population worldwide. The definite diagnosis of AD still depends on post-mortem pathological examination of amyloid plaques consisting of amyliod-β peptides (Aβ) fibrils in the brain so far. However, these fibrils are not closely linked to the development of the disease. Alternatively, soluble Aβ are believed to be more reliable biomarkers for early diagnosis of AD. Here, we report a simple approach to quantitative detection of soluble Aβ species using N-(6-(benzothiazol-2-yl)pyridin-3-yl)-5-(dimethylamino)naphthalene-1-sulfonamide (BPNS) as a ratiometric fluorescence Zn^{2+} probe. This ratiometric fluorescence assay is based on the competition of soluble Aβ with BPNS for Zn^{2+}, that is, soluble Aβ species with higher chelation affinity can capture Zn^{2+} from BPNS–Zn^{2+} adduct, thereby reactivating the ratiometric fluorescence response of BPNS. BPNS exhibited perfect linear relationship ($R^2 = 0.998$) in accordance with the concentration of soluble Aβ in the presence of Zn^{2+}. The assay possesses strong anti-interference capacity against exogenous agent or the other proteins, thanks to the high selectivity for soluble Aβ species. Importantly, this assay can quantitatively detect soluble Aβ species from different types of biological fluids, such as artificial cerebrospinal fluid (ACSF), serum, and plasma in half an hour. This assay provides a low-cost, fast, sensitive, and simple approach for quantitative detection of soluble Aβ species and may serve as a potential tool for early-stage AD diagnosis.

1. Introduction

Alzheimer's disease (AD), a devastating neurodegenerative disorder, is the most common cause for dementia, resulting in a large personal, familial, and financial burden on society (Mcdade and Bateman, 2017). More painfully, efficacious diagnosis of AD is not at hand so far, especially in the early stage of the disease, which may be the primary cause of the protracted progress in developing preventive therapeutics (Scheltens et al., 2016). Fortunately, detection of pathological factors as biomarkers has demonstrated promising potential in more accurate diagnosis of AD with increased understanding of AD pathogenesis (Blennow, 2010). Amyloid plaques consisting of amyloid-β peptides (Aβ) fibrils, the major neuropathological hallmark of AD, is currently predominant biomarker with great value in AD diagnosis (Blennow, 2010). Positron emission tomography (PET) imaging of Aβ plaques has already been in clinical use (Viola et al., 2015). However, these insoluble Aβ plaques do not correlate well with cognitive impairment in the term of both amount and location, and are not present in the earliest stages of the disease (Nyborg et al., 2013). Alternatively, soluble Aβ species, mainly as oligomers, are proposed to be more neurotoxic than insoluble Aβ fibrils, playing a central role in memory loss (Haass and Selkoe, 2007). Moreover, they appear as early as ~10–15 years before the clinical symptom of AD, allowing them as more valuable biomarkers for early diagnosis or even prognosis. However, the detection of soluble Aβ species is still challenging due to their metastable nature (Lee et al., 2017).

Unlike Aβ fibrils only existing in the brain, soluble Aβ species can also efflux into body fluids such as cerebrospinal fluid (CSF) and plasma (Wang et al., 2017). Despite at low concentration, soluble Aβ species in such body fluids have been proved to correlate with plaque burden, thus may provide the earliest clue to predict the progress of AD pathology. Currently, antibody-depended immunoassays in conjunction with routine analytical techniques, i.e., colorimetry, fluorescence, electrochemistry, are the most prevalent detection platforms for quantifying soluble Aβ species (Chan et al., 2017; Liu et al., 2013a; Carneiro et al., 2017; Zakaria et al., 2018). However, they are often costly, time-consuming, and less sensitive due to the use of expensive and less stable antibodies as receptors to capture and recognize soluble Aβ species.

* Corresponding author. College of Chemistry and Molecular Engineering, Nanjing Tech University, Nanjing, 211816, PR China.
E-mail address: wangxhui@njtech.edu.cn (X. Wang).

https://doi.org/10.1016/j.bios.2019.111518
Received 12 May 2019; Received in revised form 29 June 2019; Accepted 15 July 2019
Available online 15 July 2019
0956-5663/

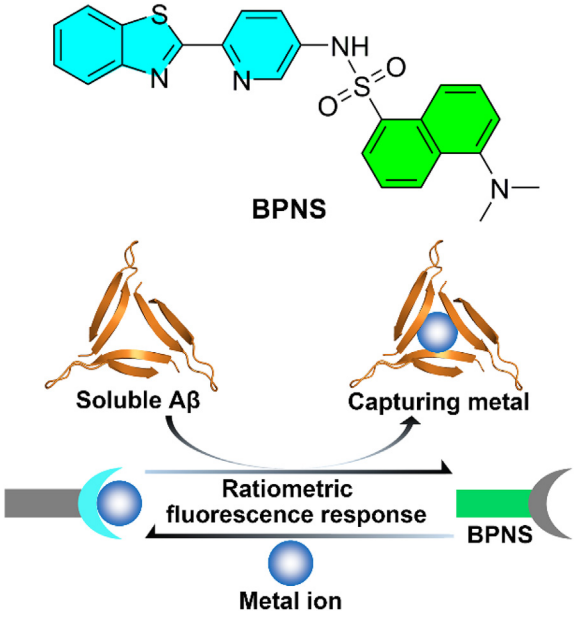

Fig. 1. The structure (top) and design principle (bottom) of BPNS.

Moreover, although a few of analytical platforms including surface plasmon resonance, mass spectrometry, and surface-enhanced Raman spectroscopy have been employed for Aβ detection with improved sensitivity (Kim et al., 2019; Ford et al., 2008; Nakamura et al., 2018), their practical applications have been hindered by the requirements of sophisticated instruments and operational expertise. To overcome the limitation of antibody-based immunoassays, ratiometric fluorescence sensing with small molecule sensors would offer an attractive option for quantitative detection due to its striking advantages, such as simplicity, low cost, high sensitivity, and inherent reliability, resulting from its self-calibration effect of two emission bands that can eliminate the interference from local probe concentration, photobleaching, as well as instrumental parameters (Lee et al., 2015). Nevertheless, only one example to date has plausibly showed ratiometric fluorescence response to soluble Aβ species, but unavailability for quantitative detection because of poor selectivity (Kim et al., 2018).

We herein construct a ratiometric fluorescence probe N-(6-(benzothiazol-2-yl)pyridin-3-yl)-5-(dimethylamino)naphthalene-1-sulfonamide (BPNS) for quantitative detection of soluble Aβ species on the basis of the competition between Aβ and chelator for a metal ion (Fig. 1). Metal ions, especially Zn^{2+} and Cu^{2+}, can bind to Aβ with high chelation affinity to promote Aβ nucleation and aggregation (Faller et al., 2014; Wang et al., 2018). Accordingly, Aβ may regulate the fluorescence of fluorescent chelators for Zn^{2+} or Cu^{2+} through coordinating with chelator-bound metal ions. Thus, BPNS, composed of two fluorophores: the metal-chelating unit 2-pyridylbenzothiazole (PBT) group and dansyl group, is supposed to give off ratiometric fluorescence response for Zn^{2+} or Cu^{2+} with lower binding affinity compared with that of soluble Aβ, thereby achieving metal-mediated ratiometric fluorescence detection of soluble Aβ upon sequestration of the metal ions from BPNS–metal adduct by the peptides (Fig. 1). As expected, soluble Aβ can selectively trigger the ratiometric fluorescence response of BPNS–Zn^{2+} adduct through capturing Zn^{2+}, enabling a quantitative detection of soluble Aβ species with strong anti-interference capacity and high reliability. To the best of our knowledge, this is the first ratiometric fluorescence assay for quantitative detection of soluble Aβ species from biological fluids.

2. Experimental

Details on experimental section were provided in the Supplementary Material.

3. Results and discussion

3.1. Design of the proposed approach

In order to achieve quantitative detection of Aβ by fluorophotometry, the common dual fluorophore-based strategy was initially adopted for rational construction of a ratiometric fluorescence probe for metal ion (Kaur and Kumar, 2011). Because the fluorescence of each chromophore would be simultaneously modulated by the communication between the two fluorophoric units triggered by the metal ion, thereby enabling a ratiometric fluorescence response for the metal ion. Meanwhile, it is essential that the binding affinity of the proposed probe for the metal ion should be lower than that of soluble Aβ. To this aim, PBT group was selected as metal chelating moiety with moderate binding affinity to Zn^{2+} or Cu^{2+} due to its bidentate scaffold (Maheswari et al., 2008). Dansyl group has been widely used to construct bifluorophoric ratiometric probes because of its robust fluorescence in visible region, large Stokes shift, and high sensitivity to the environment (Maity and Govindaraju, 2010; Chen et al., 2011). Upon addition of soluble Aβ to the solution of BPNS–metal adduct, the fluorescence of BPNS would ratiometrically recover owing to the capture of BPNS-bound metal ions by Aβ (Fig. 1). As a result, the amount of soluble Aβ in unknown samples is presumed to be determined from the relationship between fluorescence signal of BPNS and the concentration of standard soluble Aβ species. Furthermore, BPNS can be easily synthesized from common commercial reagents with two routine reactions. The synthetic route and characterization of BPNS are described in Scheme S1, Fig. S1, and S2. Therefore, it is reasonable that BPNS would be a suitable ratiometric probe to construct metal-mediated fluorescence assay for quantitative detection of soluble Aβ.

3.2. Feasibility for ratiometric recognition of soluble Aβ

To prove the feasibility of this approach, the fluorescence response of BPNS for Zn^{2+} was first investigated by fluorescence titration. When excited at the maximum excitation wavelength (332 nm), BPNS per se showed a strong fluorescence emission of dansyl group at 505 nm ($\Phi = 0.086$), accompanied with a subtle emission of the PBT moiety at 423 nm, which is mainly attributed to the efficient energy transfer (EET) from PBT part to the dansyl substructure in such bichromophoric scaffold (Saura et al., 2015). In addition, the photoinduced electron transfer (PeT) from the secondary amine of sulfonamide to PBT moiety may further quench the fluorescence of PBT (Fig. 2A) (Yang et al., 2016). Upon addition of Zn^{2+} into the BPNS solution, a remarkable decrease of fluorescence intensity at 505 nm and a concomitant increase in the intensity at 423 nm were observed, simultaneously yielding a single isosbestic point at 442 nm. This ratiometric response can be ascribed to the coordination between BPNS and Zn^{2+} to form the complex BPNS–Zn^{2+}, resulting in the blocking of PeT and EET process by the chelation-enhanced-fluorescence effect (Andréasson and Pischel, 2010; Liu et al., 2013b). The formation of BPNS–Zn^{2+} was confirmed by the absorption titration of BPNS with Zn^{2+} (Fig. S3). Zn^{2+} addition leaded to a decrease in the 336 nm absorption band, along with increase in the 415 nm absorption band. A single isosbestic point at 370 nm can be also found in Fig. S3. More importantly, the apparent association constant ($^{a}K_{a}$) of BPNS with Zn^{2+} in the 20 mM Tris buffer was determined to be $4.11 \times 10^{6}\ M^{-1}$ by nonlinear fitting to the fluorescence titration curve (Fig. S4), which is lower than that of Aβ for Zn^{2+} under the same condition (Bush et al., 1994). These results strongly indicate that BPNS–Zn^{2+} system could be served as a ratiometric probe for soluble Aβ, which is highly expected to capture Zn^{2+} out of BPNS–Zn^{2+}.

On the other hand, the binding behavior of BPNS for Cu^{2+} was also measured by both absorption and fluorescence titrations. Titration of Cu^{2+} shows a similar absorption change in the UV–visible spectrum as

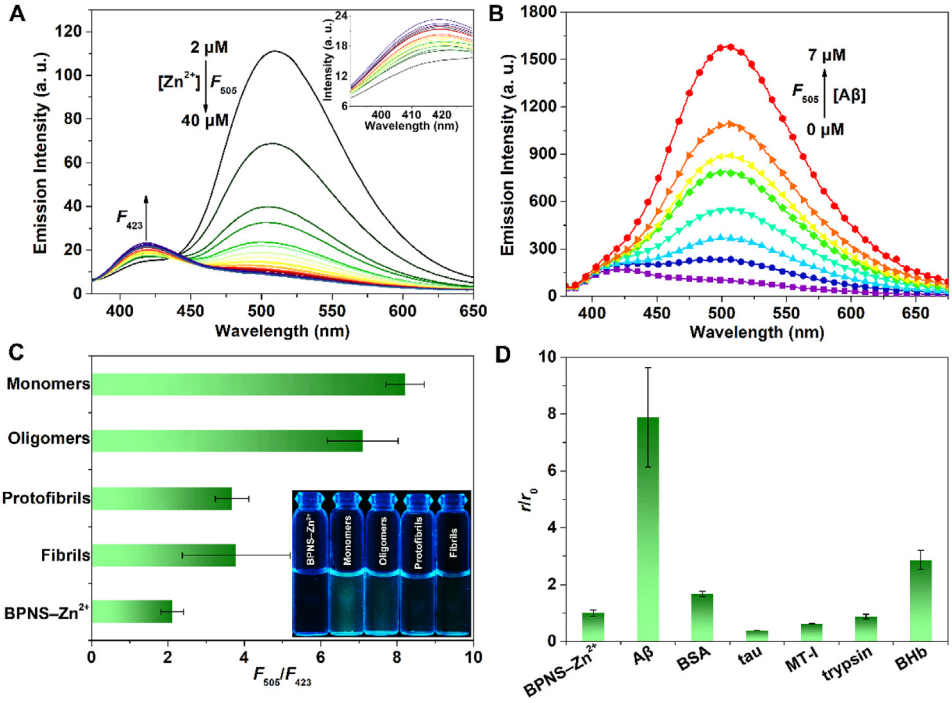

Fig. 2. The fluorescence spectra of BPNS upon addition of increasing concentration of Zn^{2+} (A) and Aβ monomer in the presence of Zn^{2+} (10 μM) (B). Inset: the closeup of fluorescence spectra in the range of 390–430 nm; The selectivity of BPNS ratiometric fluorescence for soluble Aβ species against insoluble Aβ species (C) and the other proteins (D) in the presence of Zn^{2+} (10 μM). Inset: fluorescence images of BPNS–Zn^{2+} system in the presence of different Aβ species under a UV lamp at 365 nm. The fluorescence of BPNS (20 μM, λ_{ex} = 332 nm) was measured in buffer (20 mM Tris-HCl, 150 mM NaCl, 5‰ v/v MeOH, pH 7.4). The concentration of different proteins was 20 μM. The data shown are mean values ± standard deviation, n = 3. (r and r_0 are the F_{505}/F_{423} ratio of BPNS in the presence and absence of proteins, respectively).

observed for Zn^{2+}, indicating the coordination of Cu^{2+} to the PBT group (Fig. S5). Nevertheless, both the fluorescence intensities at 423 and 505 nm were quenched by Cu^{2+} (Fig. S6), probably due to the strong paramagnetic nature of Cu^{2+} (Jung et al., 2009). Moreover, the conditional association constant (K_a) of BPNS for Cu^{2+} was calculated to be $3.87 \times 10^{10}\ M^{-1}$ using the previously obtained ^aK_a (Fig. S6), which is much higher than that of Aβ–Cu^{2+} in the same Tris buffer (Hatcher et al., 2008; Vello et al., 2010), indicating that BPNS–Cu^{2+} system is unavailable for ratiometric recognition of Aβ. Therefore, according to the metal binding properties of BPNS, the BPNS–Zn^{2+} system was properly chosen for further detection of Aβ.

As expected, in the solution of BPNS–Zn^{2+} system, the addition of Aβ40 monomer resulted in a significant recovery of the quenched emissive intensity at 505 nm, while the peak at 423 nm almost disappeared, indicating the good ratiometric responses of BPNS to Aβ monomer in the presence of Zn^{2+} (Fig. 2B). Titration experiment showed that the ratio of the emission intensity at 505 and 423 nm (F_{505}/F_{423}) gradually increase with the increasing concentration of Aβ40 monomer until 10 μM (Fig. S7). These ratiometric change could be attributed to the release of Zn^{2+} from BPNS triggered by the strong competition of Aβ monomer for binding Zn^{2+} against BPNS. As a result, the quantum yield of BPNS–Zn^{2+} solution (Φ = 0.060) also increased to 0.160 upon addition of Aβ40 monomer. Moreover, the BPNS–Zn^{2+} displayed a good linear relationship (R^2 = 0.995) between the ratios (F_{505}/F_{423}) and the concentrations of Aβ40 monomer in the range of 0–7 μM (Fig. S8), endowing BPNS with a detection limit (3σ/slope) of 390 nM for Aβ40 monomer under the test condition.

We next explored the fluorescence responses of BPNS for different Aβ species in the presence of Zn^{2+}. Aβ species at different aggregation states were prepared through pre-incubation of Aβ monomer in Tris buffer at 37 °C for different time, which were confirmed by thioflavin T (ThT) fluorescence assay using the dye ThT as a fluorescence probe of amyloid fibril (Knowles et al., 2009). Accordingly, the soluble Aβ monomers and oligomers (24 h) and the insoluble protofibrils (48 h) as well as fibrils (72 h) were selected as models in the test (Fig. S9). As Fig. 2C shows, the soluble Aβ samples can dramatically induce the ratiometric responses of BPNS–Zn^{2+} system. The effect of fluorescence change was much higher than those triggered by both insoluble protofibrils and fibrils, probably resulting from the higher binding affinity of the soluble Aβ species for Zn^{2+} than that of the insoluble counterparts (Talmard et al., 2007). Furthermore, such distinction in the fluorescence responses to the tested samples can be also visually observed by the naked eye under a UV lamp (365 nm). The nonluminous BPNS–Zn^{2+} was lighted up by the soluble Aβ species with bright green fluorescence, whereas only glimmer can be found in the systems containing the insoluble Aβ species.

The selectivity of BPNS for soluble Aβ species against the other proteins (e.g. tau protein, bovine serum albumin (BSA), bovine hemoglobin (BHb), metallothionein-I (MT-I), and trypsin) was further evaluated. As shown in Fig. 2D and S10, the proteins hardly changed the F_{505}/F_{423} ratio of BPNS in the presence of Zn^{2+}, compared with BPNS–Zn^{2+} solution as control. BPNS still exhibited excellent selectivity for soluble Aβ against the proteins with one order of magnitude higher concentration than that of Aβ (Fig. S11), implying that BPNS could be a Zn^{2+}-mediated ratiometric fluorescence probe for the soluble Aβ. In particular, almost no responses of BPNS for tau protein and BSA, one of the AD biomarkers and the most abundant interfering protein in blood, respectively (Cook et al., 2015; Wang et al., 2011), would warrant the feasibility of the ratiometric fluorescence probe to quantify soluble Aβ species in AD samples for early diagnosis.

To further understand the Zn^{2+}-mediated recognition mechanism of BPNS for soluble Aβ, the fluorescence response of BPNS for Aβ in the absence of Zn^{2+} was initially investigated. The free BPNS was unable to discriminate different Aβ species, which induced similar fluorescence enhancement of BPNS at 505 nm with up to ~3-fold, while no ratiometric response of BPNS was observed (Fig. S12). The fluorescence increase of BPNS may be attributed to the affinity of PBT moiety to Aβ (Noël et al., 2013), which would influence the EET of PBT to dansyl group. Moreover, the free BPNS also demonstrated low selectivity for Aβ against the other proteins (Fig. S13). These results forcefully validated the indispensability of Zn^{2+} in the ratiometric recognition of BPNS for soluble Aβ. Since Zn^{2+} can strikingly promote the aggregation of Aβ through coordination with His and Asp residues of Aβ (Rauk, 2009; Faller et al., 2013), the Aβ aggregation in the presence of BPNS or/and Zn^{2+} were also measured. Similar amounts of soluble Aβ species were observed in the supernatant of both BPNS-treated and free Aβ monomers with different co-incubation time by dot-blot assay using monoclonal Aβ-specific antibody 6E10 (Fig. 3A), indicating that BPNS

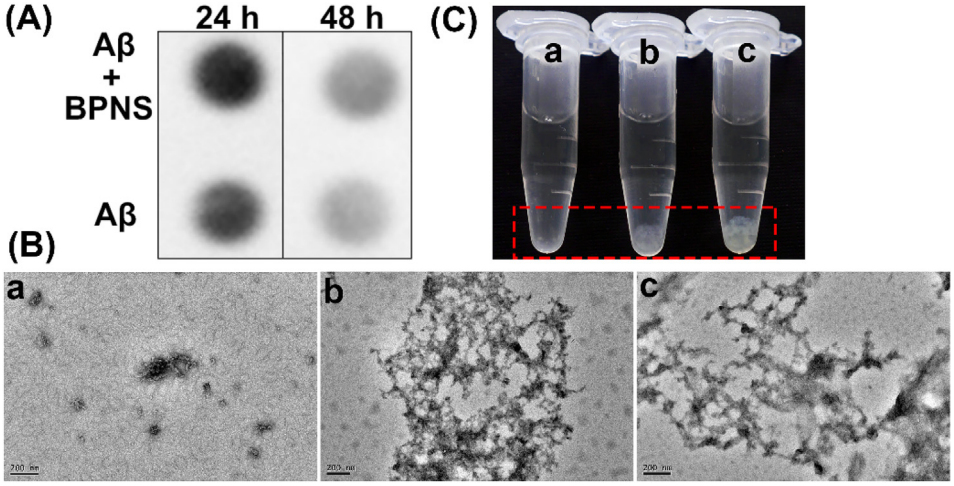

Fig. 3. (A) Dot-blot assay of BPNS-treated and untreated Aβ aggregation with different incubation time (24 h and 48 h) using monoclonal Aβ-specific antibody 6E10; TEM (B) and photographic (C) images of different Aβ samples with or without Zn^{2+} and BPNS–Zn^{2+} (a, Aβ; b, Aβ + Zn^{2+}; c, Aβ + BPNS–Zn^{2+}).

hardly impact Aβ aggregation. However, significant aggregation of Aβ took place to eventually form insoluble fibrils upon incubation with BPNS–Zn^{2+} system, which were morphologically identical with Zn^{2+}-induced Aβ aggregates under the same condition visualized by transmission electron microscopy (TEM) (Fig. 3B). In contrast, only small and short species were produced with Aβ self-aggregation under the same incubation condition. The more effective aggregation of Aβ with BPNS–Zn^{2+} or Zn^{2+} than that of free Aβ monomers was even visible with the naked eye. A large number of insoluble Aβ aggregates formed as flocculent precipitate in the tubes of Aβ with both BPNS–Zn^{2+} and Zn^{2+} (Fig. 3C). Overall, the results indicate that the soluble Aβ species can efficiently sequester Zn^{2+} from BPNS–Zn^{2+} through coordinative interactions to trigger Zn^{2+}-induced aggregation, concomitantly inducing the ratiometric fluorescence response of BPNS.

3.3. Optimization of the fluorescence assay

To maximize the detection efficacy, a series of experimental conditions were optimized. Firstly, the concentration of Zn^{2+} may influence the fluorescence assay due to the pivotal role of Zn^{2+} in the ratiometric recognition. In this regard, the fluorescence response of BPNS to Aβ monomers in the presence of 10 and 20 μM concentrations of Zn^{2+} was measured, respectively. As depicted in Fig. S14, in the case of 10 μM Zn^{2+}, the ratios showed better linear relationship with increasing concentration of Aβ in the range of 0–10 μM. Hence, the Zn^{2+} concentration of 10 μM was used in the following experiments. Since the ratiometric response of BPNS depends on the competition between BPNS and Aβ for chelating Zn^{2+}, which was monitored in the incubation process by both fluorescence and absorption spectroscopy (Fig. S15). The F_{505}/F_{423} ratio rapidly increased in the beginning of incubation until 2 h, following with a plateau, indicating the time-depended response of BPNS–Zn^{2+} for the soluble Aβ species, which was nearly consistent with the result of absorption spectra. Subsequently, the effect of co-incubation time of BPNS–Zn^{2+} with the soluble Aβ species on the detective performances was investigated. Interestingly, almost the same concentration-depended profiles were observed as the co-incubation time of 0.5, 1, and 12 h, in which the F_{505}/F_{423} ratios had good linear correlations with the concentration of Aβ monomers in the range of 0–10 μM. On the contrary, the sample without co-incubation scarcely showed the linear relationship (Fig. S16). The results indicate that 0.5 h of co-incubation was sufficient for the quantitative detection and thus was set as the co-incubation time in the assay.

On the basis of the above findings, BPNS fluorescence assay for quantifying soluble Aβ species was proposed as shown in Fig. 4. The mixture of BPNS and Zn^{2+} is prepared as working reagent (WR).

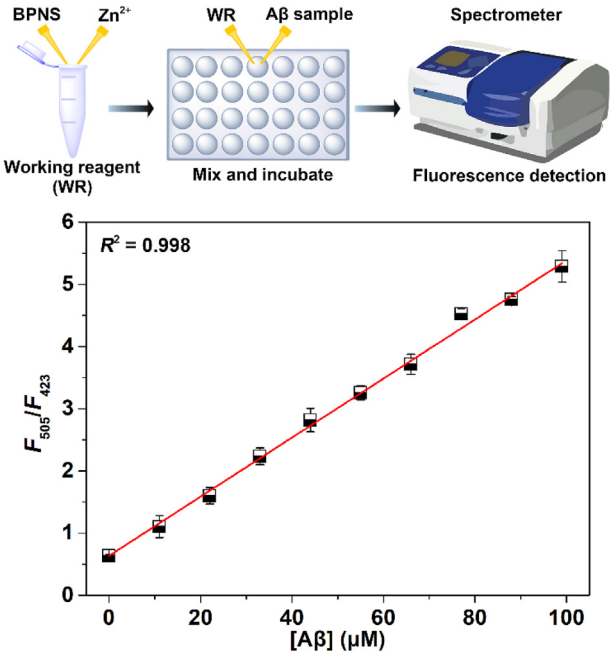

Fig. 4. Top: Schematic representation of BPNS fluorescence assay to quantitative detection of soluble Aβ. Bottom: Plot of the F_{505}/F_{423} ratio of BPNS (20 μM, λ_{ex} = 332 nm) with Zn^{2+} (10 μM) in buffer (20 mM Tris-HCl, 150 mM NaCl, 5‰ v/v MeOH, pH 7.4) as a function of Aβ standard concentrations in the range of 0–100 μM.

Considering the almost identical effect of Aβ monomers and oligomers on the fluorescence response of BPNS, a set of diluted Aβ monomers solution are selected as standards without pre-incubation. Each standard in certain volume are added into WR solution, respectively. After co-incubation for 30 min at 37 °C, the fluorescence intensities of the mixture at 423 and 505 nm are collected. Subsequently, calibration curve by plotting the F_{505}/F_{423} ratio for each Aβ standard against its concentration is obtained, which can be used to determine the soluble Aβ concentration of each unknown sample. As expected, BPNS exhibited excellent linear relationship (R^2 = 0.998) between F_{505}/F_{423} ratio and the concentration of Aβ standards in the range of 0–100 μM (Fig. 4). Thus, 0–100 μM was identified as the optimal working range of the assay for soluble Aβ species.

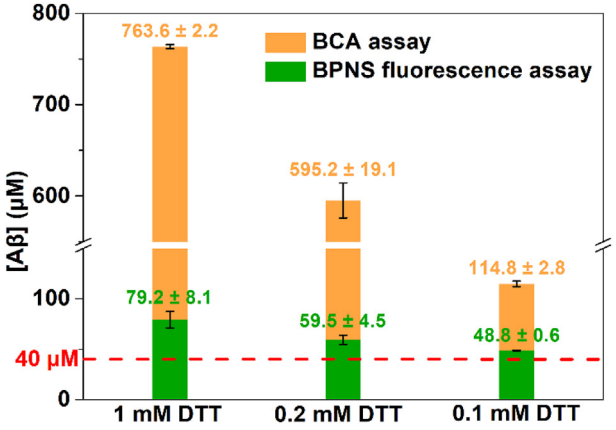

Fig. 5. The concentration of soluble Aβ determined by BCA protein assay and BPNS fluorescence assay in the presence of DTT with different concentrations.

3.4. Anti-interference capacity of the fluorescence assay

To explore the anti-interference capacity of BPNS fluorescence assay, lysozyme and MT-I were selected as interfering proteins for quantitative detection of soluble Aβ in complicated environment. As shown in Table S1, BPNS fluorescence assay showed convincing ability to quantify the soluble Aβ with excellent recoveries and good precision in the presence of both proteins, even at the high concentration of 0.5 mM in the case of MT-I. Besides the endogenous proteins, dithiothreitol (DTT), a common reducing agent in biological experiments, was also employed as an exogenous interference to explore the anti-interference capability of the assay. BCA protein assay was used as the control. DTT can dramatically disturb the detection of Aβ in BCA protein assay even at the concentration of 0.1 mM in Tris buffer (Fig. 5), by which much higher values of concentration were obtained than the calculated one (40 μM) based on the concentration of Aβ stock solution. On the contrary, the reducing agent had negligible effect on the detection of BPNS fluorescence assay at such high concentration (0.1 mM). These results verified the strong anti-inference capability of the assay, warranting its practical applications in biological samples.

3.5. Quantitative detection of soluble Aβ in biological fluids

CSF Aβ levels have already recognized as useful indices to predict the progress of AD particularly at the early stage of the disease (Blennow and Zetterberg, 2015). In addition, blood-based Aβ biomarkers have attracted more and more attention to develop cost-effective and noninvasive diagnosis of AD, owing to the routine blood collection in clinical practice (O'Bryant et al., 2017). Encouragingly, it has been experimentally affirmed that plasma Aβ possess robust correlation with both Aβ deposition in the brain and levels of Aβ in CSF, implying the potential clinical utility of blood-based Aβ biomarkers (Nakamura et al., 2018). In our work, to demonstrate the potential of the proposed assay for practical application, the levels of soluble Aβ in artificial CSF (ACSF), serum, and plasma were determined. For this purpose, Aβ solutions were initially prepared in the three fluids, respectively. The standard values of Aβ concentration in such biological fluids can be calculated from the concentrations of stock solution, which were determined by BCA assay and enzyme-linked immunosorbent assay (ELISA), respectively. The detection results were summarized in Table 1. As anticipated, BPNS fluorescence assay was able to accurately detect the concentration of soluble Aβ40 from ACSF, compared with the standard values obtained from both BCA assay and ELISA. Unfortunately, it was incompetent to quantify the Aβ in the serum and plasma, probably due to the strong interference by the background fluorescence of such complicated fluids. To solve this problem, pre-dilution of serum and plasma with Tris buffer was carried out. Accordingly, BPNS fluorescence assay can detect Aβ with satisfactory recoveries when serum and plasma were diluted to 1.25% and 1%, respectively (Table 1 and Fig. S17). Considering that dilution prior to detection is routine operation for blood samples (Wang et al., 2008; Piliarik et al., 2010), the proposed assay seems available for quantitative detection of soluble Aβ even in the biological fluids.

Table 1
Determination of soluble Aβ from ACSF, serum, and plasma by BPNS fluorescence assay.

	Standard value (55 μM) by BCA assay [a]			Standard value (35 μM) by ELISA [a]		
	Found (μM)	Recovery (%)	RSD (%)	Found (μM)	Recovery (%)	RSD (%)
ACSF	55.8	101.4	4.9	34.9	99.7	2.7
Diluted serum	57.6	104.8	6.2	34.8	99.4	2.8
Diluted plasma	57.7	104.9	4.3	35.6	101.7	2.1

[a] The standard values of Aβ concentration were calibrated by BCA assay and ELISA, respectively.

4. Conclusions

In conclusion, for the first time, we rationally designed a Zn^{2+}-mediated method for quantitative detection of soluble Aβ species using a ratiometric fluorescence probe (BPNS). As a proof of concept, BPNS gave off ratiometric fluorescence response for AD-associated Zn^{2+} with high sensitivity and selectivity, but with weaker binding affinity for Zn^{2+} than that of soluble Aβ, making it suitable as a ratiometric fluorescence probe for soluble Aβ. Soluble Aβ can capture BPNS-bound Zn^{2+} to recover BPNS fluorescence in ratiometric mode. Based on the distinctive mechanism of action, BPNS exhibited good selectivity for soluble Aβ against the insoluble counterparts as well as the other proteins in the presence of Zn^{2+}. Notably, excellent linear relationship between the ratiometric fluorescence signal of BPNS and the concentration of soluble Aβ was obtained, indicating the feasibility of BPNS fluorescence assay for quantifying soluble Aβ. Using the proposed assay, quantitative detection of soluble Aβ can be achieved in the Tris buffer with some interferences and in biological fluids including ACSF, diluted serum and plasma in short time. Considering the facile and low-cost preparation, fast response with high sensitivity, and simple operation, this approach would be potentially used as a tool for early diagnosis of AD. Although BPNS would be unavailable for determination of Aβ in AD samples at picomolar concentrations due to its insufficient detection limit, the promising results of this work warrant pursuit of optimizations of this approach through structural modifications of the ratiometric fluorescence probe, that are ongoing in our group.

Declaration of competing interest

The authors declare that they have no known competing financial interests or personal relationships that could have appeared to influence the work reported in this paper.

CRediT authorship contribution statement

Changhong Li: Formal analysis, Writing - original draft. **Liu Yang:** Formal analysis. **Xiaohui Wang:** Formal analysis, Writing - original draft.

Acknowledgements

We appreciate the financial support from the National Natural Science Foundation of China (Grants: 21771105 and 21301090), the Natural Science Foundation of Jiangsu Province (Grant: BK20170103),

the Natural Science Foundation of the Jiangsu Higher Education Institutions (Grant: 17KJB150018), and the Six Talent Peaks Project in Jiangsu Province (Grant: SWYY-043).

Appendix A. Supplementary data

Supplementary data to this article can be found online at https://doi.org/10.1016/j.bios.2019.111518.

References

Andréasson, J., Pischel, U., 2010. Chem. Soc. Rev. 39 (1), 174–188.
Blennow, K., 2010. Nat. Med. 16 (11), 1218–1222.
Blennow, K., Zetterberg, H., 2015. Nat. Med. 21 (3), 217–219.
Bush, A.I., Pettingell, W.H., Paradis, M.D., Tanzi, R.E., 1994. J. Biol. Chem. 269 (16), 12152–12158.
Carneiro, P., Loureiro, J., Delerue-Matos, C., Morais, S., do Carmo Pereira, M., 2017. Sens. Actuators B Chem. 239, 157–165.
Chan, H.-N., Xu, D., Ho, S.-L., Wong, M.S., Li, H.-W., 2017. Chem. Sci. 8 (5), 4012–4018.
Chen, L., Yang, L., Li, H., Gao, Y., Deng, D., Wu, Y., Ma, L.-j., 2011. Inorg. Chem. 50 (20), 10028–10032.
Cook, C., Murray, M.E., Petrucelli, L., 2015. Nat. Med. 21 (3), 219–220.
Faller, P., Hureau, C., Berthoumieu, O., 2013. Inorg. Chem. 52 (21), 12193–12206.
Faller, P., Hureau, C., La Penna, G., 2014. Acc. Chem. Res. 47 (8), 2252–2259.
Ford, M.J., Cantone, J.L., Polson, C., Toyn, J.H., Meredith, J.E., Drexler, D.M., 2008. J. Neurosci. Methods 168 (2), 465–474.
Haass, C., Selkoe, D.J., 2007. Nat. Rev. Mol. Cell Biol. 8 (2), 101–112.
Hatcher, L.Q., Hong, L., Bush, W.D., Carducci, T., Simon, J.D., 2008. J. Phys. Chem. B 112 (27), 8160–8164.
Jung, H.S., Kwon, P.S., Lee, J.W., Kim, J.I., Hong, C.S., Kim, J.W., Yan, S., Lee, J.Y., Lee, J.H., Joo, T., Kim, J.S., 2009. J. Am. Chem. Soc. 131 (5), 2008–2012.
Kaur, K., Kumar, S., 2011. Dalton Trans. 40 (11), 2451–2458.
Kim, H.S., Lee, S.H., Choi, I., 2019. Analyst 144 (8), 2820–2826.
Kim, S., Lee, H.J., Nam, E., Jeong, D., Cho, J., Lim, M.H., You, Y., 2018. ACS Omega 3 (5), 5141–5154.
Knowles, T.P.J., Waudby, C.A., Devlin, G.L., Cohen, S.I.A., Aguzzi, A., Vendruscolo, M., Terentjev, E.M., Welland, M.E., Dobson, C.M., 2009. Science 326 (5959), 1533–1537.
Lee, M.H., Kim, J.S., Sessler, J.L., 2015. Chem. Soc. Rev. 44 (13), 4185–4191.
Lee, S.J.C., Nam, E., Lee, H.J., Savelieff, M.G., Lim, M.H., 2017. Chem. Soc. Rev. 46 (2), 310–323.
Liu, L., Zhao, F., Ma, F., Zhang, L., Yang, S., Xia, N., 2013a. Biosens. Bioelectron. 49, 231–235.
Liu, Z., He, W., Guo, Z., 2013b. Chem. Soc. Rev. 42 (4), 1568–1600.
Maheswari, P.U., Ster, M.v.d., Smulders, S., Barends, S., Wezel, G.P.v., Massera, C., Roy, S., Dulk, H.d., Gamez, P., Reedijk, J., 2008. Inorg. Chem. 47 (9), 3719–3727.
Maity, D., Govindaraju, T., 2010. Chem. Commun. 46 (25), 4499–4501.
Mcdade, E., Bateman, R.J., 2017. Nature 547 (7662), 153–155.
Nakamura, A., Kaneko, N., Villemagne, V.L., Kato, T., Doecke, J.D., Dore, V., Fowler, C., Li, Q., Martins, R.N., Rowe, C., 2018. Nature 554 (7691), 249–254.
Noël, S., Cadet, S., Gras, E., Hureau, C., 2013. Chem. Soc. Rev. 42 (19), 7747–7762.
Nyborg, A.C., Moll, J.R., Wegrzyn, R., Havas, D., Hutterpaier, B., Feuerstein, G.Z., Rudolph, A.S., 2013. J. Alzheimer's Dis. 34 (4), 957–967.
O'Bryant, S.E., Mielke, M.M., Rissman, R.A., Lista, S., Vanderstichele, H., Zetterberg, H., Lewczuk, P., Posner, H., Hall, J., Johnson, L., Fong, Y.-L., Luthman, J., Jeromin, A., Batrla-Utermann, R., Villarreal, A., Britton, G., Snyder, P.J., Henriksen, K., Grammas, P., Gupta, V., Martins, R., Hampel, H., 2017. Alzheimer's Dementia 13 (1), 45–58.
Piliarik, M., Bocková, M., Homola, J., 2010. Biosens. Bioelectron. 26 (4), 1656–1661.
Rauk, A., 2009. Chem. Soc. Rev. 38 (9), 2698–2715.
Saura, A.V., Marín, M.J., Burguete, M.I., Russell, D.A., Galindo, F., Luis, S.V., 2015. Org. Biomol. Chem. 13 (28), 7736–7749.
Scheltens, P., Blennow, K., Breteler, M.M.B., de Strooper, B., Frisoni, G.B., Salloway, S., Van der Flier, W.M., 2016. Lancet 388 (10043), 505–517.
Talmard, C., Bouzan, A., Faller, P., 2007. Biochemistry 46 (47), 13658–13666.
Vello, T.U., Ann, K., Peep, P., 2010. J. Neurochem. 104 (5), 1249–1259.
Viola, K.L., Sbarboro, J., Sureka, R., De, M., Bicca, M.A., Wang, J., Vasavada, S., Satpathy, S., Wu, S., Joshi, H.M., 2015. Nat. Nanotechnol. 10 (1), 91–98.
Wang, J., Gu, B.J., Masters, C.L., Wang, Y., 2017. Nat. Rev. Neurol. 13 (10), 612–623.
Wang, X., Wang, X., Guo, Z., 2018. Coord. Chem. Rev. 362, 72–84.
Wang, X., Wang, X., Wang, Y., Guo, Z., 2011. Chem. Commun. 47 (28), 8127–8129.
Wang, Y., Qian, W., Tan, Y., Ding, S., 2008. Biosens. Bioelectron. 23 (7), 1166–1170.
Yang, T., Yang, L., Zhang, C., Wang, Y., Ma, X., Wang, K., Luo, J., Yao, C., Wang, X., Wang, X., 2016. Inorg. Chem. Front. 3 (12), 1572–1581.
Zakaria, N., Ramli, M.Z., Ramasamy, K., Meng, L.S., Yean, C.Y., Banga Singh, K.K., Zain, Z.M., Low, K.-F., 2018. Anal. Biochem. 555, 12–21.